1

Fundamentals

1.1 ADAPTIVE COMMUNICATIONS AND THE BOOK LAYOUT

In order to justify the content of the book and to make suggestions on how the book should be studied, we start with the generic block diagram of a digital communication system shown in Figure 1.1.

The standard building blocks, information source, source encoder, encryptor, channel encoder and data modulator are used to produce a narrowband signal, for example, binary phase shift keying (BPSK), quaternary phase shift keying (QPSK) or M-ary quadrature amplitude modulation MQAM carrying information content. The spreading of the signal spectra is obtained by real or complex multiplication of the narrowband signal by a code. After power amplification, the signal will be transmitted by one antenna or by multiple antennae (transmit diversity). After multipath propagation, multiple replica of the transmitted signal will reach the receiver. In a number of parallel processors (RAKE), the receiver will try to independently demodulate a number of signal replicas. The first step is signal despreading of the number of multipath components. To do so a channel estimator is needed to estimate the delays and amplitudes of these components in order to be optimally combined in coherent RAKE combiner. Prior to combining, cancelation of multiple access and multipath interference (MPI) may be performed in order to improve system performance. After signal combining, the remaining signal processing, including channel decoder, decryptor and source decoder, is performed. Separate block 'channel + network' characterizes the impact of fading, noise, network design and information broadcast from the network for control purposes.

On the basis of side information obtained either from the network or channel estimator, the *receiver configuration control* block from Figure 1.1 will put together the best possible receiver/transmitter parameters or even change the system configuration.

Coding The most powerful coding is obtained by using concatenated codes with interleavers that are known under the name *turbo codes*. The algorithm that iteratively decodes 'turbo' codes was first proposed by Berrou *et al*. [1]. It is also explained in detail by Hagenauer *et al*. [2]. A general iterative algorithm applicable to all forms of code concatenations

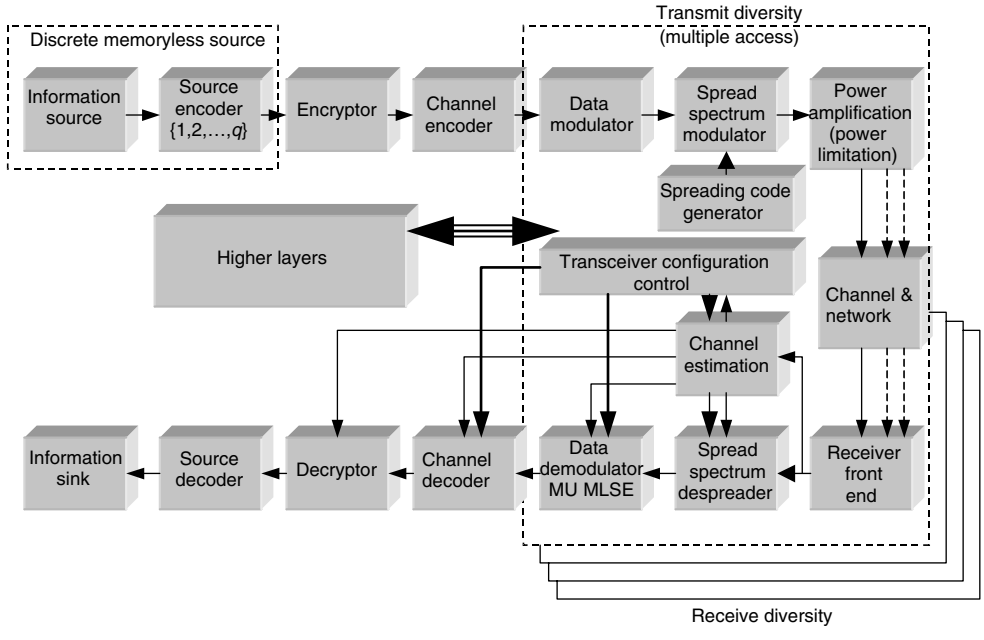

Figure 1.1 Generic block diagram of a digital communication system.

has been described by Benedetto *et al.* [3]. A number of papers have appeared on the subject of the 'turbo' iterative decoding algorithms, showing that it can be viewed as an instance of previously proposed algorithms (see, for example, Reference [4] and the extensive references therein). To avoid a huge reference list, the readers are referred to the papers and references in the *European Transactions on Telecommunications* [5], and in the *IEEE Journal on Selected Areas in Communications* [6], entirely devoted to concatenated codes and iterative decoding.

Coded modulation It has been generally accepted that modulation and coding should be combined in a single entity for improved performance. Of late, the increasing interest in mobile radio channels has led to the consideration of coded modulation for fading channels. Thus, at first blush it seemed quite natural to apply 'Ungerboeck's paradigm' of keeping coding combined with modulation even in the Rayleigh fading channel, in which the code performance depends strongly on the code minimum Hamming distance (the 'code diversity'), rather than on its minimum Euclidean distance. Several results followed this line of thought, as documented by a considerable body of work summarized and referenced in Reference [7] (see also Reference [8], Chapter 10). Under the assumption that the symbols were interleaved with a depth exceeding the coherence time of the fading process, new codes were designed for the fading channel so as to maximize their diversity.

A notable departure from Ungerboeck's paradigm was the core of Reference [9]. Schemes were designed aimed at keeping as their basic engine an off-the-shelf Viterbi

decoder for the *de facto* standard, 64-state rate-1/2 convolutional code. This implied giving up the joint decoder/demodulator in favor of two separate entities.

On the basis of the latter concept, Zehavi [10] recognized that the code diversity, and hence the reliability of coded modulation over a Rayleigh fading channel, could be further improved. Zehavi's idea was to make the code diversity equal to the smallest number of distinct *bits* (rather than *channel symbols*) along any error event. This is achieved by bit-wise interleaving at the encoder output, and by using an appropriate soft-decision bit metric as an input to the Viterbi decoder. Further results along this line were recently reported in References [11–13] (for different approaches to the problem of designing coded modulation schemes for the fading channels, see References [14,15]).

Of particular interest is paper [16] based on Zehavi's findings, and in particular on his rather surprising *a priori* result that on some channels there is a downside to combining demodulation and decoding. The paper presents the theory underlying bit-interleaved coded modulation (BICM) comprehensively, and provides a general information-theoretical framework for this concept.

It also provides results for a large range of the signal constellation QPSK-256 QAM.

Adaptive coded modulation After the signal despreading point in Figure 1.1, we assume a flat-fading channel with additive white Gaussian noise (AWGN) $n(t)$ and a stationary and ergodic channel gain $\sqrt{[g(t)]}$. Let $\overline{S}$ denote the average transmit signal power, $N_0/2$ denotes the noise density of $n(t)$, B denotes the received signal bandwidth, and $\overline{g}$ denotes the average channel gain. With appropriate scaling of $\overline{S}$, we can assume that $\overline{g} = 1$. For a constant transmit power $\overline{S}$, the instantaneous received signal-to-noise ratio (SNR) is $\gamma(t) = \overline{S}g(t)/(N_0B)$ and the average received SNR is $\overline{\gamma} = \overline{S}/(N_0B)$. We denote the fading distribution of γ by $p(\gamma)$. If the transmit power $S(t)$ is adapted relative to $g(t)$ or, equivalently, to $\gamma(t)$, then the SNR at time t is given by

$$SNR(t) = \frac{\gamma(t)S[\gamma(t)]}{\overline{S}} = \frac{g(t)S[g(t)]}{N_0B}$$

In accordance with Reference [17], adaptive coded modulation does not require interleaving, since error bursts are eliminated by adjusting the power, size and duration of the transmitted signal constellation, relative to the channel fading. In general, we would rather like to include the interleaver in the block 'channel encoder' in Figure 1.1. For fast fading, in which adaptation is less effective, the interleaving should help. For slow fading, in which adaptation is more effective, the interleaver cannot do much but neither does it do any damage.

However, adaptive modulation does require accurate channel estimates at the receiver, which are fed back to the transmitter with minimal latency. The effects of estimation error and feedback path delay on adaptive modulation were analyzed in Reference [18], in which it was found that an estimation error less than 1 dB and a feedback path delay less than $0.001/f_D$ results in minimal performance degradation, for $f_D = v/\lambda$ the Doppler frequency of the fading channel. The effect of estimation error and feedback path delay for adaptive coded modulation is similar, yielding the same set of requirements for minimal performance degradation. These requirements are easily met on slowly varying channels.

Another practical consideration in adaptive coded modulation scheme is how quickly the transmitter must change its constellation size. Since the constellation size is adapted to an estimate of the channel fade level, several symbol times may be required to obtain a good estimate. In addition, hardware and pulse-shaping considerations generally dictate that the constellation size must remain constant over tens to hundreds of symbols. It was shown in Reference [18] that this requirement translates mathematically to the requirement that $\overline{\tau}_j \gg \mathrm{T}\ \forall j$, where T is the symbol for time and $\overline{\tau}_j$ is the average time when the adaptive modulation scheme continuously uses the constellation M_j. Since each constellation M_j is associated with a range of fading values called the fading region $R_j, \overline{\tau}_j$ is the average time that the fading stays within the region R_j. The value of $\overline{\tau}_j$ is inversely proportional to the channel Doppler and also depends on the number and characteristics of the different fade regions. It was shown in Reference [18] that in Rayleigh fading with an average SNR of 20 dB and a channel Doppler of 100 Hz, $\overline{\tau}_j$ ranges between 0.7 and 3.9 ms, and thus for a symbol rate of 100 ksymbols s^{-1}, the signal constellation remains constant over tens to hundreds of symbols. Similar results hold at other SNR values.

In a narrowband system, the flat-fading assumption in this model implies that the signal bandwidth B is much less than the channel coherence bandwidth $B_c = 1/T_M$, where T_M is the root-mean-square (rms) delay spread of the channel. For Nyquist pulses $B = 1/T$, so flat fading occurs when $T \gg T_M$. Combining $T \gg T_M$ and $\overline{\tau}_j \gg T$, we see that $\overline{\tau}_j \gg T \gg T_M$ must be satisfied to have both flat fading and the signal constellation constant over a large number of symbols. In general, wireless channels have rms delay spreads less than 30 μs in outdoor urban areas and less than around 1 μs in indoor environments [19]. Taking the minimum $\overline{\tau}_j = 0.7$ ms, we see that on the basis of the previous relation, rates on the order of tens of ksymbols per second in outdoor channels and hundreds of ksymbols per second in indoor channels are practical for this adaptive scheme.

For WCDMA, these conditions will be extensively discussed throughout the book, especially later on in this chapter and then in much more detail in Chapter 8.

Coset codes with adaptive modulation Reference [17] shows how the separability of code and modulation design inherent in coset codes can be used to combine coset codes with adaptive modulation. A binary encoder E, from Figure 1.1, operates on k uncoded data bits to produce $k + r$ coded bits, and then the coset (subset) selector uses these coded bits to choose one of the 2^{k+r} cosets from a partition of the signal constellation. In nonadaptive modulation dealt with in Reference [20], the *modulation* segment uses $n - k$ additional uncoded bits to choose one of the 2^{n-k} signal points in the selected coset, which is then transmitted via the modulator. These steps essentially decouple the channel coding from the modulation. Specifically, the fundamental coding gain is a function of the minimum squared distance between signal point sequences, which is determined by the encoder (E) properties and the subset partitioning, independent of the modulation. This minimum distance is given by $d_{\min} = \min\{d_{\mathrm{s}}, d_{\mathrm{c}}\}$, where d_{s} is the minimum distance between coset sequences and d_{c} is the minimum distance between coset points. For square MQAM signal constellations, both d_{s} and d_{c} are proportional to d_0, the minimum distance between constellation points before partitioning. The number of nearest neighbor code words also impacts the effective coding gain.

In a fading channel, the instantaneous SNR varies with time, which will cause the distance $d_0(t)$ in the received signal constellation, and, therefore, the corresponding distances $d_c(t)$ and $d_s(t)$, to vary. The basic premise for using adaptive modulation with coset codes is to keep these distances constant by varying the size $M(\gamma)$, transmit power $S(\gamma)$, and/or symbol time $T(\gamma)$ of the transmitted signal constellation relative to γ, subject to an average transmit power constraint $\overline{S}$ on $S(\gamma)$. By maintaining $\min\{d_c(t), d_s(t)\} = d_{\min}$ constant, the adaptive coded modulation exhibits the same coding gain as a coded modulation designed for an AWGN channel with minimum code word distance $d_{\min}$.

The *modulation* segment on Figure 1.1 would work as follows. The channel is assumed to be slowly fading so that $\gamma(t)$ is relatively constant over many symbol periods. During a given symbol period $T(\gamma)$, the size of each coset is limited to $2^{n(\gamma)-k}$, where $n(\gamma)$ and $T(\gamma)$ are functions of the channel SNR γ. A signal point in the selected coset is chosen using $n(\gamma) - k$ uncoded data bits. The selected point in the selected coset is one of $M(\gamma) = 2^{n(\gamma)+r}$ points in the transmit signal constellation [e.g. MQAM, M-ary phase-shift keying (MPSK)]. By using appropriate functions for $M(\gamma)$, $S(\gamma)$ and $T(\gamma)$, we can maintain a fixed distance between points in the received signal constellation $M(\gamma)$ corresponding to the desired minimum distance $d_{\min}$. The variation of $M(\gamma)$ relative to γ causes the information rate to vary, so the uncoded bits used for signal point selection must be buffered until needed. Since r redundant bits are used for the channel coding, $\log_2 M(\gamma) - r$ bits are sent over the symbol period $T(\gamma)$ for a received SNR of γ. The average rate of the adaptive scheme is thus given by

$$R = \int_{\gamma_0}^{\infty} \frac{1}{T(\gamma)} [\log_2 M(\gamma) - r] p(\gamma)\, \mathrm{d}\gamma$$

where $\gamma_0 \geq 0$ is a cutoff fade depth below which transmission is suspended ($M(\gamma) = 0$). This cutoff value is a parameter of the adaptive modulation scheme. Since γ is known to both the transmitter and the receiver, the modulation, encoding, and decoding processes are suspended while $\gamma < \gamma$o.

At the receiver, the adaptive modulation is first demodulated, which yields a sequence of received constellation points. Then the points within each coset that are closest to these received points are determined. From these points, the maximum-likelihood coset sequence is calculated and the uncoded bits from the channel coding segment are determined from this sequence in the same manner as for nonadaptive coded modulation in AWGN. The uncoded bits from the *modulation* segment are then determined by finding the points in the maximum-likelihood coset sequence that are closest to the received constellation points and by applying standard demodulation to these points.

The adaptive modulation described above consists of any mapping from γ to a constellation size $M(\gamma)$, power $S(\gamma)$, and symbol time $T(\gamma)$ for which $d_{\min}(t)$ remains constant. Proposed techniques for adaptive modulation maintain this constant distance through adaptive variation of the transmitted power level [21], symbol time [22], constellation size [23,24], or any combination of these parameters [18,25,26]. The *modulation* segment of Figure 1.1 can use any of these adaptive modulation methods.

Adaptive coding scheme Efficient error control on time-varying channels can be performed, independent of modulation, by implementing an adaptive control system in which the optimum code is selected according to the actual channel conditions.

There are a number of burst error-correcting codes that could be used in these adaptive schemes. Three major classes of burst error-correcting codes are binary Fire block codes, binary Iwadare–Massey convolutional codes [27], and nonbinary Reed–Solomon block codes. In practical communication systems, these are decoded by hard-decision decoding methods. Performance evaluation based on experimental data from satellite mobile communication channels [28] shows that the convolutional codes with the soft-decision decoding Viterbi algorithm are superior to all the above burst error-correcting codes of the respective rates.

Superior error probability performance and availability of a wide range of code rates without changing the basic coded structure motivate the use of punctured convolutional codes [29–32] with the soft-decision Viterbi decoding algorithm in the proposed adaptive scheme. To obtain the full benefit of the Viterbi algorithm on bursty channels, ideal interleaving is assumed.

An adaptive coding scheme using incremental redundancy in a hybrid automatic-repeat-request (ARQ) error control system is reported in Reference [33]. The channel model used is binary symmetric channel (BSC) with time variable bit error probability. The system state is chosen according to the channel bit error rate (BER). The error correction is performed by shortened cyclic codes with variable degrees of shortening. When the channel BER increases, the system generates additional party bits for error correction.

An Forward Error Correction (FEC) adaptive scheme for matching the code to the prevailing channel conditions was reported in Reference [34]. The method is based on convolutional codes with Viterbi decoding and consists of combining noisy packets to obtain a packet with a code rate low enough (less than $1/2$) to achieve the specified error rate. Other schemes that use a form of adaptive decoding are reported in References [35–40]. Hybrid ARQ schemes based on convolutional codes with sequential decoding on a memoryless channel were reported in References [41,42] while a Type-II hybrid ARQ scheme formed by concatenation of convolutional codes with block codes was evaluated on a channel represented by two states [43].

In order to implement the adaptive coding scheme, it is necessary again to use a return channel. The channel state estimator (CSE) determines the current channel state, on the basis of the number of erroneous blocks. Once the channel state has been estimated, a decision is made by the *reconfiguration block* whether to change the code, and the corresponding messages are sent to the encoder and locally to the decoder.

In FEC schemes, only error correction is performed, while in hybrid ARQ schemes retransmission of erroneous blocks is requested whenever the decoded data is labeled as unreliable.

The adaptive error protection is obtained by changing the code rates. For practical purposes, it is desirable to modify the code rates without changing the basic structure of the encoder and decoder. Punctured convolutional codes are ideally suited for this application. They allow almost continuous change of the code rates while decoding is done by the same decoder.

The encoded digits at the output of the encoder are periodically deleted according to the deleting map, specified for each code. Changing the number of deleted digits varies the code rate. At the receiver end, the Viterbi decoder operates on the trellis of the parent code and uses the same deleting map as in the encoder in computing path metrics [30].

The Viterbi algorithm based on this metric is a maximum-likelihood algorithm on channels with Gaussian noise since on these channels the most probable errors occur between signals that are closest together in terms of squared Euclidean distance. However, this metric is not optimal for non-Gaussian channels. The Viterbi algorithm allows use of channel state information for fading channels [44].

However, a disadvantage of punctured convolutional codes compared to other convolutional codes with the same rate and memory order is that error paths are typically long. This requires quite long decision depths of the Viterbi decoder.

A scheme with ARQ rate-compatible convolutional codes was reported in Reference [32]. In this scheme, rate-compatible codes are applied. The rate compatibility constraint increases the system throughput since in transition from higher to lower rate codes, only incremental redundancy digits are retransmitted. The error detection is performed by a cyclic redundancy check, which introduces additional redundancy.

Adaptive coding, modulation and power control While adaptive modulation (with coded or uncoded signal) and adaptive coding described earlier are conceptually well understood and elaborated, joint adaptation of coding and modulation still remains a challenge, especially from the practical point of view. The third element of the adaptation will be power control. For details on power control algorithms and extensive literature overview, the reader is referred to Chapter 6 of the book and to Reference [45]. Capacity of the cellular network with power control, including impact of power control imperfections on the system's performance, is discussed in Chapters 8 and 9.

Adaptive frequency and space domain interference cancelation Narrowband interference generated by intentional jamming (military applications) or by belonging to other systems [such as the time division multiple access (TDMA) network] may be suppressed either in frequency or space domain. Adaptive interference suppression in frequency domain is discussed in Chapter 7 with focus on possible overlay of WCDMA macro and TDMA micro cellular networks. For space domain interference suppression and capacity improvements based on adaptive antenna arrays, the reader is referred to References [46–49].

Adaptive packet length Adaptive coding combined with ARQ described earlier would require reconfiguration of layer 2 (different format for each retransmission). An additional step to be considered is to use a variable packet length including the information segment so that possibilities for additional improvements are obtained. These algorithms are discussed in Chapter 12.

Adaptive spreading factor Depending on the level of interference, an adaptive selection of the interference suppression capabilities, measured by the system processing gain, can

be adopted to continuously provide the best trade-off between the BER and information rate. For the fixed bandwidth available, this is equivalent to bit rate adaptation.

Adaptation in time, space and frequency domain The concept of adaptive modulation and coding can be extended to frequency and space domain, resulting in adaptive multicarrier modulation with space diversity. For space-time coding, the reader is referred to References [50–52].

RAKE reconfiguration Coming back to Figure 1.1, the additional element of system adaptation and reconfigurability is the RAKE receiver itself. In time-varying multipath fading, the receiver will be constantly searching for the stronger components in the received signal than those being combined. Any time when such a component is found, the reassignment of the RAKE finger to the new one would take place. RAKE finger acquisition and reacquisition, and tracking in delay and space domain are discussed in Chapters 3 and 4 of the book.

Intertechnology adaptation If intertechnology roaming is assumed, and the receiver is supposed to be used in cellular and ad hoc networks, the reconfiguration in the signal format and consequently in transmitter and receiver structure would take place. A whole additional family of Code Division Multiple Access (CDMA) signal formats for application in ad hoc networks is discussed in Chapter 15. The extension of these formats to ultrawideband (UWB) technology is straightforward. The only difference is that instead of bipolar sequence, a unipolar (on–off) sequence should be used for signal spreading. For UWB technology, the reader is referred to References [53–57]. This concept can be extended to include reconfiguration of CDMA into TDMA type of receiver or reconfiguration of CDMA receiver for different standards such as the WCDMA and the cdma2000. Practical solutions are based on software radio [58].

Minimum complexity (energy consumption) adaptation In order to save energy, an adaptive receiver would be continuously trying to minimize the complexity of the receiver. For example, coding or multiuser detectors would be used only in the case in which the channel [including fading and multiple access interference (MAI)] is not good enough. So that required quality of service (QoS) cannot be provided without these components. As an example, multiuser detectors, described in Chapters 13 and 14 can be only occasionally used in the receiver. This would also require corresponding reconfiguration of the receiver. Practical solutions for such options are discussed in Chapter 17 for use in Universal Mobile Telecommunication System (UMTS) standard.

Adaptive access control Adaptation on the medium access control (MAC) layer would include access control. The access control mechanism is supposed to keep the number of simultaneously transmitting users in the network below or up to the system capacity. In WCDMA networks, this capacity varies in time as a result of the time-varying channel and the number of users in the surrounding cells. An adaptive system would

continuously monitor these conditions and update the capacity threshold for access control. Adaptive algorithms based on fuzzy logic and Kalman filters are discussed in detail in Chapters 10, 11, and 12.

Adaptive routing Adaptation on the network layer would include adaptive routing in wireless network. The best available segments of the multihop rout are chosen in order to minimize retransmissions and guarantee QoS [59–74].

Adaptive source coding If adaptive routing and techniques in the physical link level control and MAC layer cannot provide the required QoS, the grade of service (GoS) can be reduced, for example, by reducing the source bit rate. Variable bit rate source encoder would be constantly adapting to the conditions in the network.

Adaptive/reconfigurable network architecture The latest concepts of telecommunications networks suggest even the evolution of network flexibility in the domain of network architecture. The communications network infrastructure would consist of a network of powerful computers and an operator would be able to rent a part of the network and establish its own network architecture depending on the market at the time. It would be able to change it in time as the market changes so that network architecture would be reconfigurable from the point of view of the operator. These issues are considered in the field of active and reprogrammable networks. To keep the list of references short, the reader is referred to Reference [75]. In ad hoc networks, the network reconfigurability adapts to the mobility and activity of the nodes [67,69,72,73].

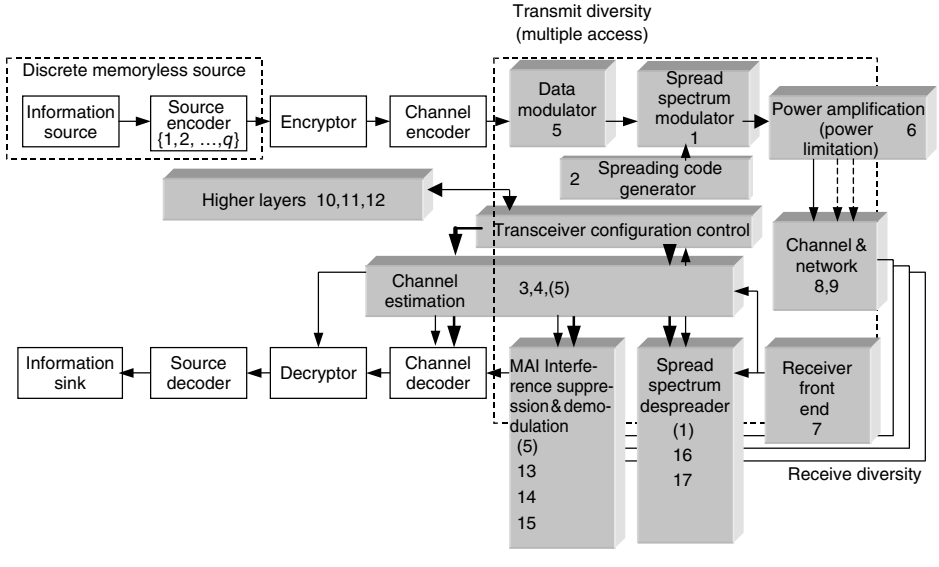

Figure 1.2 Generic block diagram of a digital communication system and book layout.

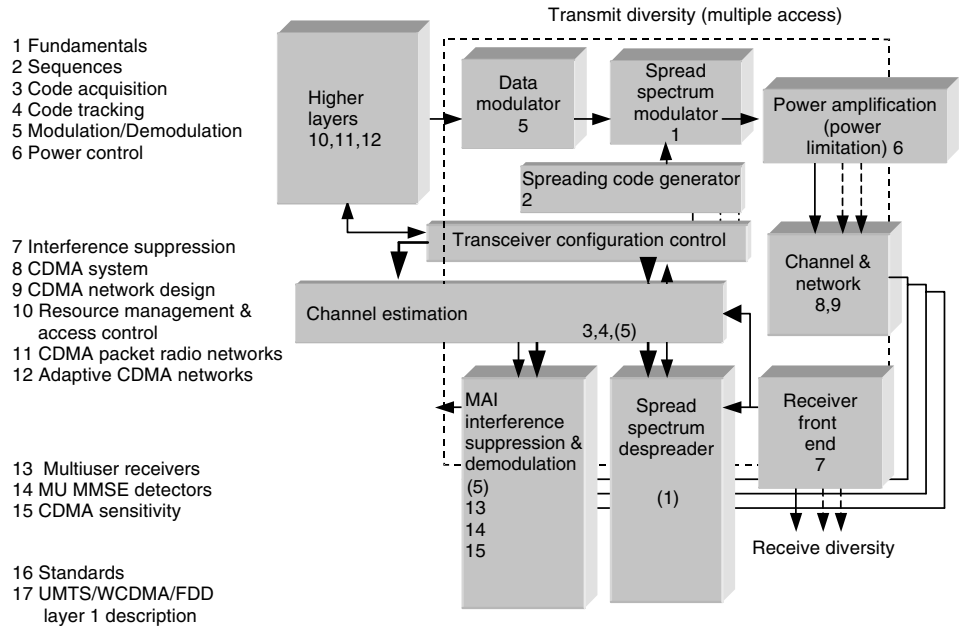

Figure 1.3 Book layout.

In this book, we cover the subsets of the problems listed above. Figure 1.2 relates to the chapters of the book and the system block diagram. Nonshaded blocks are considered as elements of the traditional communication system and are not covered in this book. For adaptive coding and modulation, the reader is referred to Reference [76]. The chapters from the book content are allocated to the respective blocks of the system, except those chapters that cover standards that cannot be allocated to specific blocks. On the left-hand side of Figure 1.3, the list of content is partitioned into four segments ***r*** – receiver, ***n*** – network, ***ar*** – advanced receiver and ***s*** – standard. This should help the reader to easily identify the specific chapters of the book. The general suggestions for the course material selections are: ***r*** – university undergraduate course on physical layer, $\boldsymbol{r} + \boldsymbol{ar}$ – university postgraduate course on physical layer, ***n*** – part of university undergraduate/postgraduate course on networks, $\boldsymbol{r} + \boldsymbol{ar} + \boldsymbol{s}$ – industry course on physical layer, $\boldsymbol{n} + \boldsymbol{s}$ – part of industry course on networks.

1.2 SPREAD SPECTRUM FUNDAMENTALS

1.2.1 Direct sequence (DS) spread spectrum

The narrowband signal in this case is a phase-shift keying (PSK) signal of the form

$$S_n = b(t, T_m) \cos \omega t \tag{1.1}$$

where $1/T_m$ is the bit rate and $b = \pm 1$ is the information. The baseband equivalent of equation (1.1) is

$$S_n^b = b(t, T_m) \tag{1.1a}$$

Spreading operation, presented symbolically by operator $\varepsilon(\ )$, is obtained if we multiply the narrowband signal by a pseudonoise (PN) sequence (code) $c(t, T_c) = \pm 1$. The bits of the sequence are called chips and the chip rate $1/T_c \gg 1/T_m$. The wideband signal can be represented as

$$S_w = \varepsilon(S_n) = cS_n = c(t, T_c)\ b(t, T_m) \cos \omega t \tag{1.2}$$

The baseband equivalent of equation (1.2) is

$$S_w^b = c(t, T_c)b(t, T_m) \tag{1.2a}$$

Despreading, represented by operator $D(\ )$, is performed if we use $\varepsilon(\ )$ once again and band-pass filtering, with the bandwidth proportional to $2/T_m$, represented by operator $BPF(\ )$ resulting in

$$\mathrm{D}(S_w) = BPF(\varepsilon(S_w)) = BPF(cc\ b \cos \omega t) = BPF(c^2\, b\ \cos \omega t) = b\ \cos \omega t \tag{1.3}$$

The baseband equivalent of equation (1.3) is

$$\begin{aligned} D(S_w^b) &= LPF(\varepsilon(S_w^b)) = LPF(c(t, T_c)c(t, T_c)b(t, T_m)) \\ &= LPF(b(t, T_m)) = b(t, T_m) \end{aligned} \tag{1.3a}$$

where $LPF(\ )$ stands for low pass filtering. This approximates the operation of correlating the input signal with the locally generated replica of the code $\mathrm{Cor}(c, S_w)$. Nonsynchronized despreading would result in

$$D_\tau(\ );\ \mathrm{Cor}(c_\tau, S_w) = BPF(\varepsilon_\tau(S_w)) = BPF(c_\tau c\ b \cos \omega t) = \rho(\tau)\, b\ \cos \omega t \tag{1.4}$$

The baseband equivalent of equation (1.4) is

$$D_\tau(\ );\ \mathrm{Cor}(c_\tau, S_w^b) = \int_0^{T_m} c_\tau S_w^b\ \mathrm{d}t = b(t, T_m) \int_0^{T_m} c_\tau c\ \mathrm{d}t = b\rho(\tau) \tag{1.4a}$$

This operation would extract the useful signal b as long as $\tau \cong 0$, otherwise the signal will be suppressed because, as we will show in Chapter 2, $\rho(\tau) \cong 0$ for $\tau \geq T_c$. Separation of multipath components in a RAKE receiver is based on this effect. In other words, if the received signal consists of two delayed replicas of the form

$$r = S_w^b(t) + S_w^b(t - \tau)$$

the despreading process defined by equation (1.4a) would result in

$$D_\tau(\ );\ \mathrm{Cor}(c,r) = \int_0^{T_m} cr\ \mathrm{d}t = b(t,T_m)\int_0^{T_m} c(c+c_\tau)\ \mathrm{d}t = b\rho(0) + b\rho(\tau)$$

Now, if $\rho(\tau) \cong 0$ for $\tau \geq T_c$, all multipath components reaching the receiver with a delay larger then the chip interval will be suppressed. If the signal transmitted by user y is despread in receiver x, the result is

$$D_{xy}(\ );\mathrm{BPF}(\varepsilon_{xy}(S_w)) = \mathrm{BPF}(c_x\, c_y\, b_y \cos\omega t) = \rho_{xy}(t)\, b_y\ \cos\omega t \tag{1.5}$$

So, in order to suppress the signals belonging to other users (multiple access interference – MAI), the cross-correlation functions should be low. In other words, if the received signal consists of the useful signal plus the interfering signal from the other user

$$r = S^b_{wx}(t) + S^b_{wy}(t) = b_x c_x + b_y c_y$$

the despreading process at the receiver of user x would produce

$$\begin{aligned} D_{xy}(\ );\ \mathrm{Cor}(c_x,r) &= \int_0^{T_m} c_x r\ \mathrm{d}t = b_x \int_0^{T_m} c_x c_x\ \mathrm{d}t + b_y \int_0^{T_m} c_x c_y\ \mathrm{d}t \\ &= b_x\rho_x(0) + b_y\rho_{xy}(0) \end{aligned}$$

When the system is properly synchronized $\rho_x(0) \cong 1$, and if $\rho_{xy}(0) \cong 0$, the second component representing MAI will be suppressed. In addition, the size of the set of codes should be large in order to be able to allocate different codes to the large number of different users. A block diagram of the BPSK DS spread-spectrum transmitter is shown in Figure 1.4 and the receiver in Figure 1.5.

If QPSK signal is used as a narrowband signal, the general form of the transmitter will be as shown in Figure 1.6 and the receiver will be as shown in Figure 1.7.

$$S_w(t) = b_1(t)c_1(t)\cos\omega_0 t + b_2(t)c_2(t)\sin\omega_0 t \tag{1.6}$$

For MQAM modulation, b_i would have $\log_2 M$ different values.

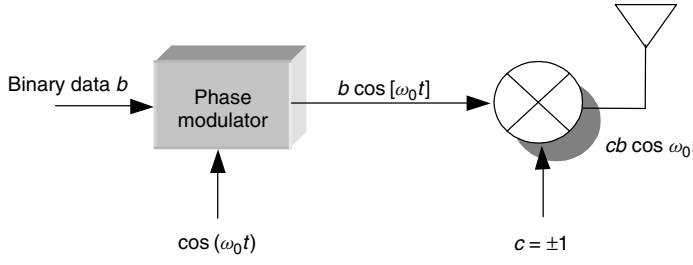

Figure 1.4 BPSK DS spread-spectrum transmitter.

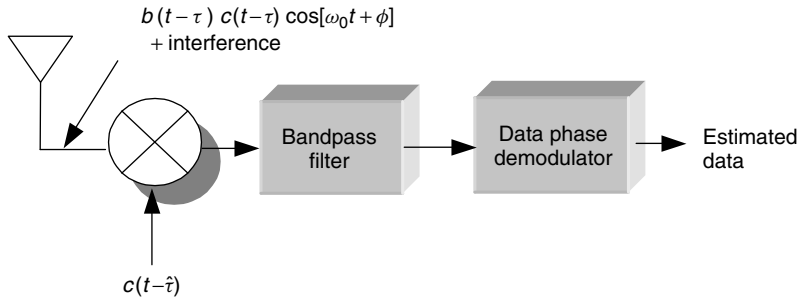

Figure 1.5 BPSK DS spread-spectrum receiver.

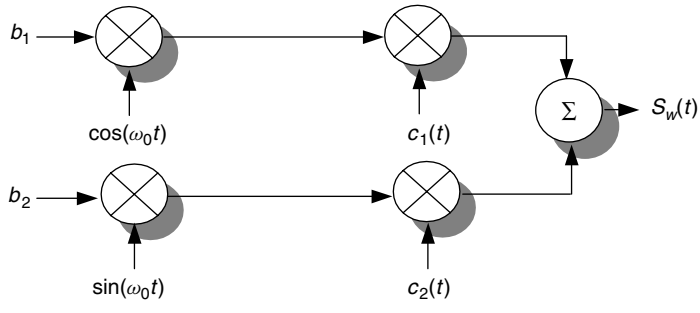

Figure 1.6 Transmitter for QPSK-DS system.

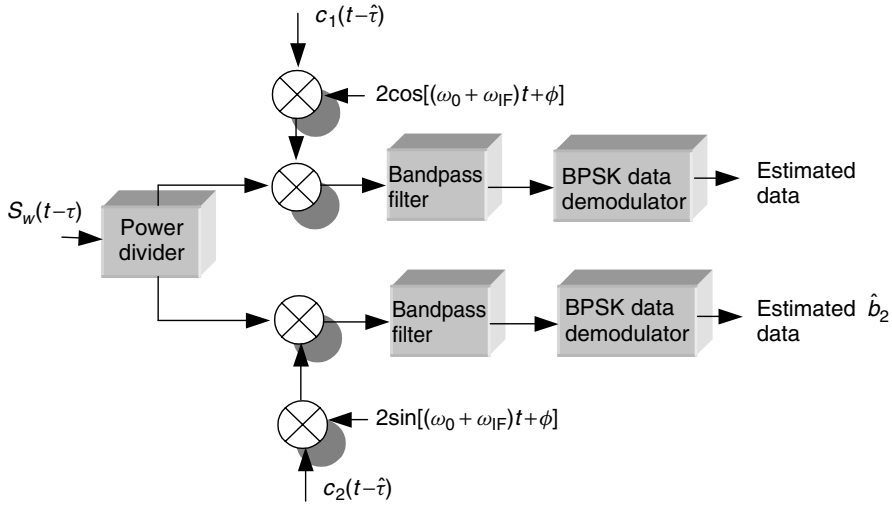

Figure 1.7 Receiver for QPSK-DS system.

If the kth transmitter sends the signal of the form given by equation (1.7) after propagation through the multipath channel, the overall received signal will have the form given by equation (1.8) where index 'lk' stands for path l of user k. As an example, the despreading process for user '$k = 1$' synchronized on path $l = 1$, will produce signal y_{11} given by equation (1.9). The first component of equation (1.9) represents a useful signal and the rest of it (double sum term) represents the MAI plus MPI. In a RAKE receiver, user $k = 1$ would separately process L signals producing $y_{l1}, l = 1, \ldots, L$. After despreading, it would have to synchronize frequency $\omega + \omega_{dlk}$ and phase θ_{lk} and after coherent demodulation get $\beta_{l1}b_1$ components to be combined in the combiner prior to final decision. The interfering terms are proportional to $\rho_{1,k}(\Delta\tau_{11,lk})$. For this reason, the codes should be designed to minimize the cross-correlation function between different users, and the autocorrelation function for $\Delta\tau \geq T_c$ to minimize the interference between the paths of the same user.

In order to improve the demodulation condition, it may use interference cancelation to remove the second term of equation (1.9) in each branch (finger) of the RAKE receiver. This problem will be discussed in Chapter 13 on multiuser detection. The block diagram of the receiver based on this concept is shown in Figures 1.8 and 1.9.

$$s_t(t) = b_k c_k \cos \omega t \tag{1.7}$$

$$r(t) = \sum_{l} \sum_{k} \beta_{lk} b_k (t - \tau_{lk}) c(t - \tau_{lk}) \cos[(\omega + \omega_{dlk})t + \theta_{lk}] \tag{1.8}$$

$$y_{11} = \beta_{11} b_1 (t - \tau_{11}) \cos[(\omega_{\text{IF}} + \omega_{d11})t + \theta_{11}] + \sum_{\substack{l \\ l,k \neq 1,1}} \sum_{k} \beta_{lk} b_k (t - \tau_{lk}) \rho_{1,k}(\Delta\tau_{11,lk}) \cos[(\omega_{\text{IF}} + \omega_{dlk})t + \theta_{lk}] \tag{1.9}$$

Using complex-envelope representation, shown in Figure 1.10 one can, in general, more precisely represent the oversimplified baseband equations (1.1a to 4a). The transmitted

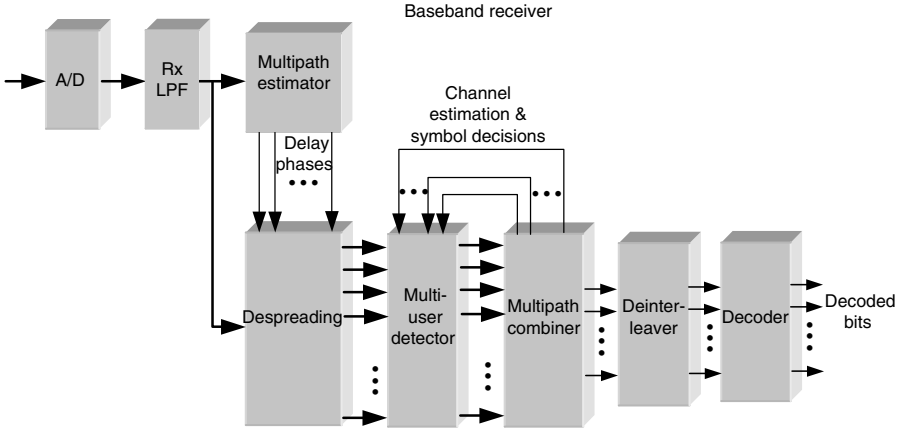

Figure 1.8 Generic receiver block diagram with optional interference cancelation stage.

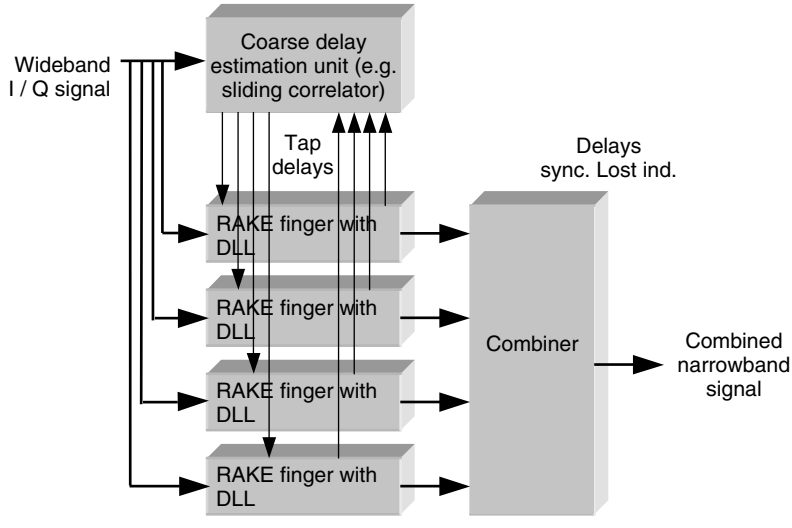

Figure 1.9 Traditional RAKE with delay lock loop (DLL) in each finger.

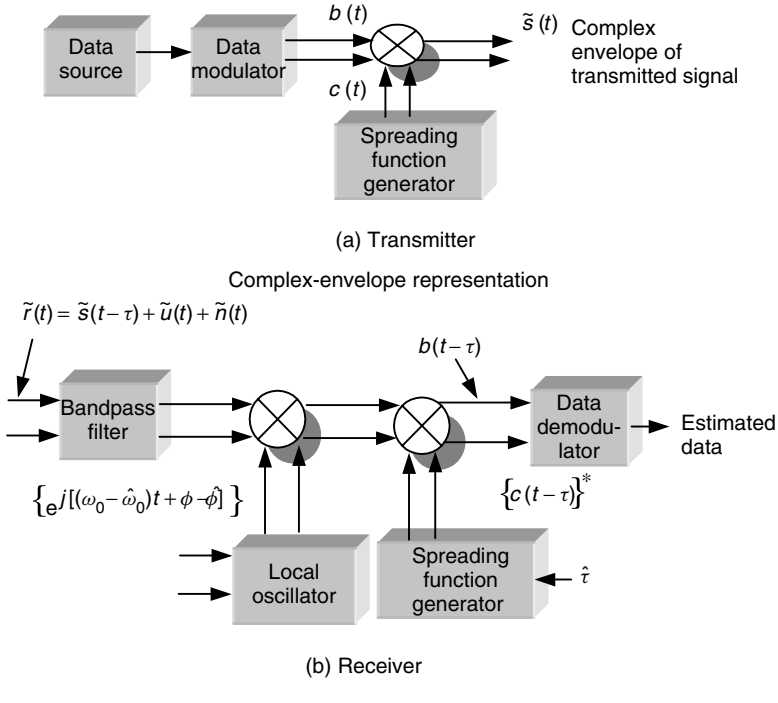

Figure 1.10 Generic complex envelope model of spread spectrum modem.

signal is represented by equation (1.10). The despread complex signal is represented by equation (1.11).

$$s(t) = \mathrm{Re}\lfloor \tilde{s}(t) \mathrm{e}^{j\omega_0 t} \rfloor \tag{1.10}$$

$$\begin{aligned} b(t-\tau) = {} & b(t-\tau)c(t-\tau)c^*(t-\hat{\tau}) \exp\{-j[(\omega_0 - \hat{\omega}_0)t + \varphi - \hat{\varphi}]\} \\ & + \tilde{u}(t)c^*(t-\tau) \exp\{-j[(\omega_0 - \hat{\omega}_0)t + \varphi - \hat{\varphi}]\} \\ & + \tilde{n}(t)c^*(t-\tau) \exp\{-j[(\omega_0 - \hat{\omega}_0)t + \varphi - \hat{\varphi}]\} \end{aligned} \tag{1.11}$$

1.3 THEORY VERSUS PRACTICE

This section provides an initial illustration on how the previous concept is implemented for multiplexing/spreading of dedicated physical data channel (DPDCH) and dedicated physical control channel (DPCCH) in universal mobile telecommunication system (UMTS). A detailed discussion of the UMTS standard is given in Chapter 17 and References [77–86]. Figure 1.11 shows the uplink DPDCH/DPCCH multiplexing and spreading for the most common case of only one DPDCH. A combination of code and IQ (In phase + Quadrature) multiplex is used, where the DPDCH and DPCCH are spread by different channelization orthogonal variable spreading factor (OVSF) codes (c_D, c_C) and mapped to an I and Q branch, respectively. The complex $I + jQ$ signal is then scrambled by a short code C_{scramb}. A short scrambling code is used in order to simplify the future implementation of advanced receiver structures, for example, multiuser detectors. As an option, long-code scrambling may be used, in the case when the base station (BS) employs ordinary RAKE reception.

1.3.1 Multicode transmission

Additional DPDCHs can be mapped to either the I or the Q branch as illustrated in Figure 1.12. Each DPDCH should be allocated to the I or Q branch in such a way that the overall envelope variations are minimized. Any IQ imbalance is avoided with the

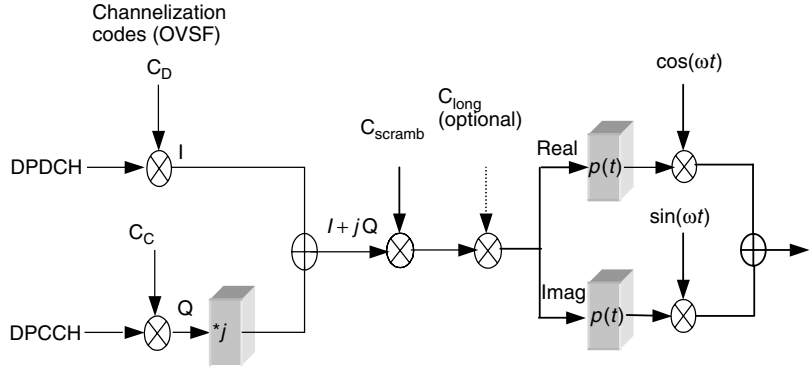

Figure 1.11 Uplink spreading and scrambling for the normal case of one DPDCH per connection.

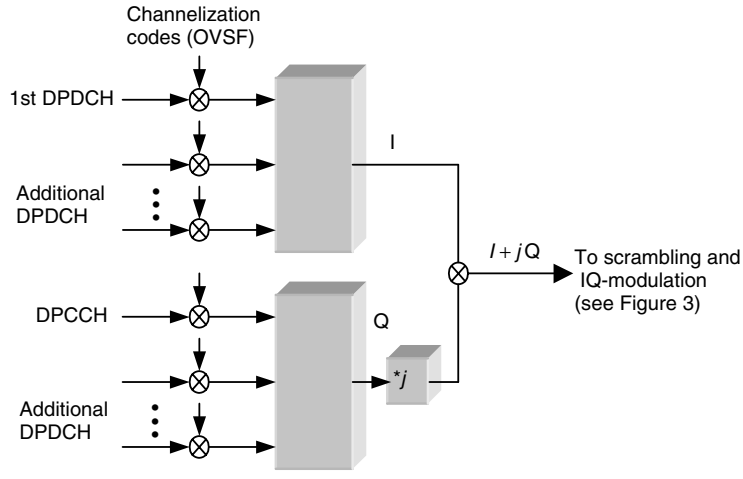

Figure 1.12 Multiplexing of multiple DPDCH on one connection (multicode transmission).

complex scrambling operation that makes the amplifier constellation similar to that with I and Q branches of equal power.

1.3.2 The downlink multiplexing and spreading

The processing is similar to that of the uplink, except that all downlink (DL) connections of a BS share a common set of short OVSF channelization codes and are jointly scrambled by a short BS unique scrambling code as shown in Figure 1.13. The BS unique scrambling code is allocated from the set of orthogonal Gold codes of length 256 chips.

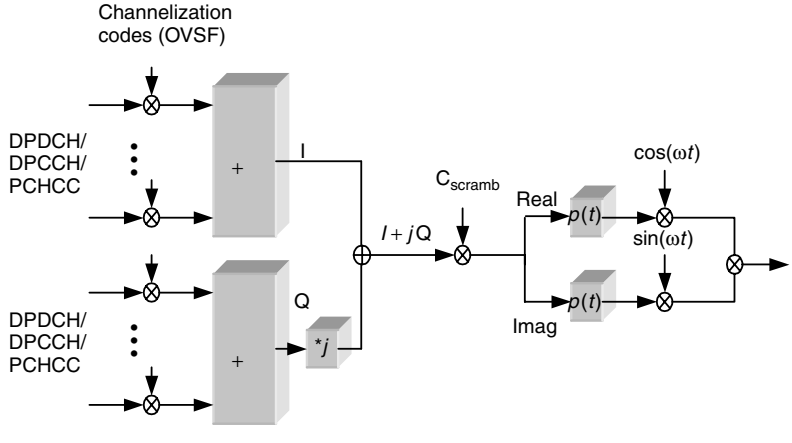

Figure 1.13 Downlink channel multiplexing and spreading.

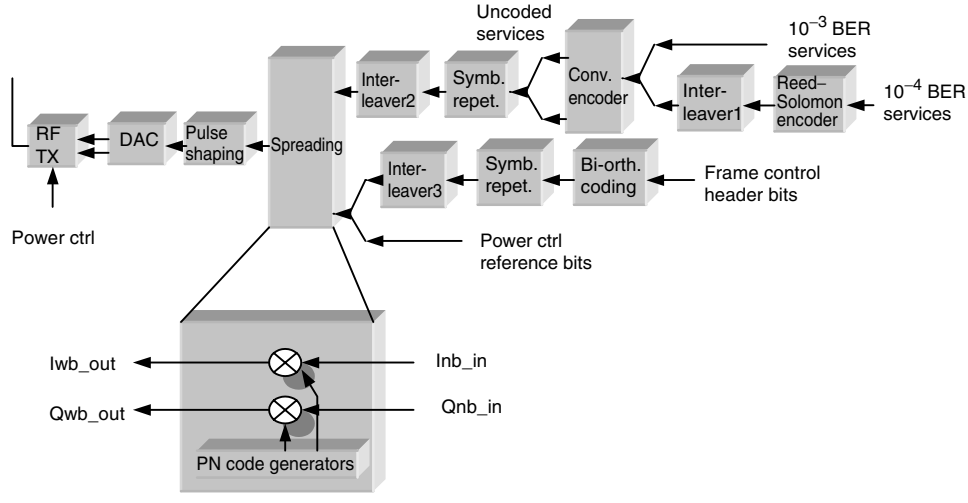

Figure 1.14 Mobile transmitter section (index wb-wideband, nb-narrowband).

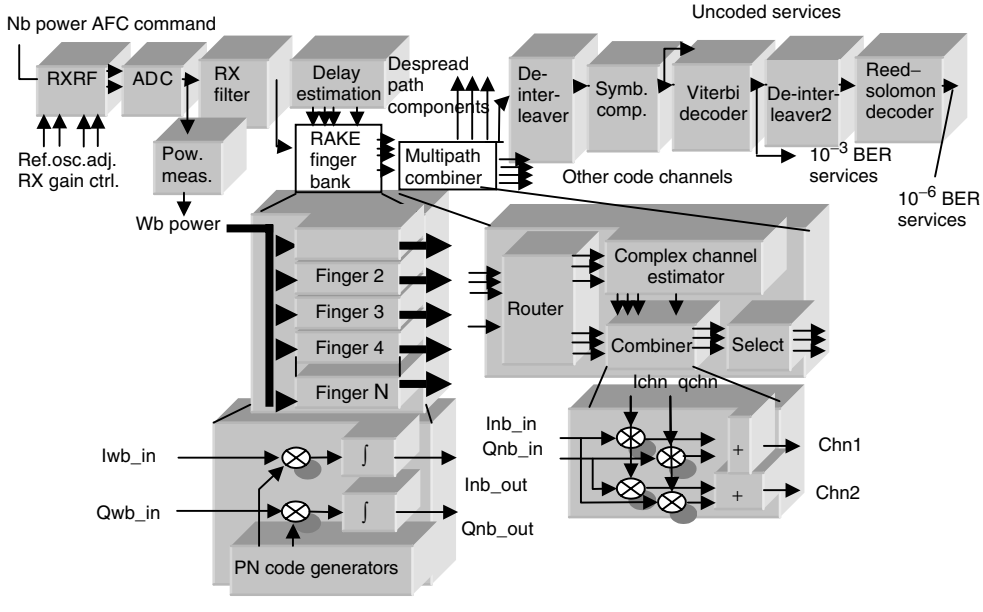

Figure 1.15 Mobile terminal receiver baseband section.

Finally, on the basis of the previous discussion, a block diagram of the mobile transmitter and receiver is shown in Figures 1.14 and 1.15, respectively. The building blocks will be discussed in detail throughout the book.

REFERENCES

1. Berrou, C. and Glavieux, A. (1996) Near optimum error-correcting coding and decoding: turbo codes. *IEEE Trans. Commun.*, **COM-44**, 1261–1271.
2. Hagenauer, J., Offer, E. and Papke, L. (1996) Iterative decoding of binary block and convolutional codes. *IEEE Trans. Inform. Theory*, **IT-42**, 429–445.
3. Benedetto, S., Divsalar, D., Montorsi, G. and Pollara, F. (1998c) Soft-input soft-output modules for the construction and distributed iterative decoding of code networks. *Eur. Trans. Telecommun.*, **9**, 155–172.
4. McEliece, R. J., MacKay, D. J. C. and Cheng, J. F. (1998) Turbo decoding as an instance of Pearl's 'Belief Propagation' algorithm. *IEEE J. Select. Areas Commun.*, **16**, 140–152.
5. Biglieri, E. and Hagenauer, J. (eds) (1995) *Eur. Trans. Telecommun.*, **6**, the whole issue.
6. Benedetto, S., Divsalar, D. and Hagenauer, J. (eds) (1998d) Concatenated coding techniques and iterative decoding: sailing toward channel capacity. *IEEE J. Select. Areas Commun.*, **16**(2), the whole issue.
7. Jamali, S. H. and Le-Ngoc, T. (1994) *Coded-Modulation Techniques for Fading Channels*. New York: Kluwer.
8. Biglieri, E., Divsalar, D., McLane, P. J. and Simon, M. K. (1991) *Introduction to Trellis-Coded Modulation with Applications*. New York: MacMillan Publishing.
9. Viterbi, A. J., Wolf, J. K., Zehavi, E. and Padovani, R. A. (1989) Pragmatic approach to trellis-coded modulation. *IEEE Commun. Mag.*, **27**, 11–19.
10. Zehavi, E. (1992) 8-PSK trellis codes for a Rayleigh channel. *IEEE Trans. Commun.*, **40**, 873–884.
11. Aoyama, A., Yamazato, T., Katayama, M. and Ogawa, A. (1994) Performance of 16-QAM with increased diversity on Rayleigh fading channels. *Proc. International Symposium on Information Theory and Its Applications*, Sydney, Australia, November 20–24, 1994, pp. 1133–1137.
12. Hansson, U. and Aulin, T. (1996) Channel symbol expansion diversity – improved coded modulation for the Rayleigh fading channel. *Presented at the International Conference on Communications*, *ICC '96*, Dallas, TX, June 23–27, 1996.
13. Al-Semari, S. A. and Fuja, T. (1996) Bit interleaved I-Q TCM. *ISITA '96*, Victoria, B.C., September 17–20, 1996.
14. Ventura-Traveset, J., Caire, G., Biglieri, E. and Taricco, G. (1997) Impact of diversity reception on fading channels with coded modulation. Part I: coherent detection. *IEEE Trans. Commun.*, **45**, 563–572.
15. Boutros, J., Viterbo, E., Rastello, C. and Belfiore, J.-C. (1996) Good lattice constellations for both Rayleigh fading and Gaussian channels. *IEEE Trans. Inform. Theory*, **42**, 502–518.
16. Caire, G. *et al*. (1998) Bit interleaved coded modulation. *IEEE Trans. Inform. Theory*, **44**(3), 927–945.
17. Goldsmith, A. *et al*. (1998) Adaptive coded modulation for fading channels. *IEEE Trans. Commun.*, **46**(5), 595–602.
18. Goldsmith, A. J. and Chua, S.-G. (1997) Variable-rate variable-power MQAM for fading channels. *IEEE Trans. Commun.*, **45**, 1218–1230.
19. Rappaport, T. S. (1996) *Wireless Communication Principles and Practice*. Englewood Cliffs, NJ: Prentice-Hall.
20. Forney Jr, G. D., Gallager, R. G., Lang, G. R., Longstaff, F. M. and Quereshi, S. U. (1984) Efficient modulation for band-limited channels. *IEEE J. Select. Areas Commun.*, **SAC-2**, 632–647.

21. Hayes, J. F. (1968) Adaptive feedback communications. *IEEE Trans. Commun.*, **COM-16**, 29–34.
22. Cavers, J. K. (1972) Variable-rate transmission for Rayleigh fading channels. *IEEE Trans. Commun.*, **COM-20**, 15–22.
23. Webb, W. T. and Steele, R. (1995) Variable rate QAM for mobile radio. *IEEE Trans. Commun.*, **43**, 2223–2230.
24. Kamio, Y., Sampei, S., Sasaoka, H. and Morinaga, N. (1995) Performance of modulation-level-controlled adaptive-modulation under limited transmission delay time for land mobile communications. *Proc. IEEE VTC '95*, July 1995, pp. 221–225.
25. Alamouti, S. M. and Kallel, S. (1994) Adaptive trellis-coded multiple-phased-shift keying for Rayleigh fading channels. *IEEE Trans. Commun.*, **42**, 2305–2314.
26. Matsuoka, H., Sampei, S., Morinaga, N. and Kamio, Y. (1996) Symbol rate and modulation level controlled adaptive modulation/TDMA/TDD for personal communication systems. *Proc. IEEE VTC '95*, April 1996, pp. 487–491.
27. Lin, S. and Costello, D. (1982) *Error Control Coding: Fundamentals and Applications*. Englewood Cliffs, NJ: Prentice Hall.
28. Gordon, N., Vucetic, B., Musicki, D. and Du, J. Joint error control and speech coding for 4.8 kbps digital voice transmission over satellite mobile channels. Tech. Rep., Sydney University, Sydney, Australia.
29. Cain, J. B., Clark, G. C. and Geist, J. M. (1979) Punctured convolutional codes of rate $(n-1)/n$ and simplified maximum likelihood decoding. *IEEE Trans. Inform. Theory*, **IT-25**, 97–100.
30. Yasuda, Y., Hirata, Y., Nakamura, K. and Otani, S. (1983) Development of variable-rate Viterbi decoder and its performance characteristics. *Proc. Sixth International Conference on Digital Satellite Communications*, Phoenix, AZ, September 1983, pp. XII-24–XII-31.
31. Yasuda, Y., Kashiki, K. and Hirata, Y. (1984) High rate punctured convolutional codes for soft decision Viterbi decoding. *IEEE Trans. Commun.*, **COM-32**, 315–319.
32. Hagenauer, J. (1988) Rate-compatible punctured convolutional codes (RCPC codes) and their applications. *IEEE Trans. Commun.*, **36**, 389–400.
33. Wu, K., Lin, S. and Miller, M. (1982) A hybrid ARQ scheme using multiple shortened cyclic codes. *Proc. GLOBECOM*, Miami, FL, pp. C8.61–C8.65.
34. Chase, D. (1985) Code combining – a maximum likelihood decoding approach for combining an arbitrary number of noisy packets. *IEEE Trans. Commun.*, **COM-33**, 385–393.
35. Sovetov, B. and Stah, V. (1982) *Design of Adaptive Transmission Systems*. Leningrad: Energoizdal; in Russian.
36. Sullivan, D. (1971) A generalization of Gallager's adaptive error control scheme. *IEEE Trans. Inform. Theory*, **IT-17**, 727–735.
37. Mandelbaum, D. (1974) An adaptive-feedback coding scheme using incremental redundancy. *IEEE Trans. Inform. Theory*, **IT-20**, 388–389.
38. Vucetic, B., Drajic, D. and Perisic, D. (1988) An algorithm for adaptive error control system synthesis. *ISIT 1985*, Brighton, UK, pp. 85–94; also in Proc. IEE, Part F Feb.
39. Mandelbaum, D. M. (1975) On forward error correction with adaptive decoding. *IEEE Trans. Inform. Theory*, **IT-21**, 230–233.
40. Kallel, S. and Haccoun, D. (1988) Sequential decoding with ARQ code combining: a robust hybrid FEC/ARQ system. *IEEE Trans. Commun.*, **26**, 773–780.
41. Drukarev, A. and Costello Jr, D. J. (1983) Hybrid ARQ control using sequential decoding. *IEEE Trans. Inform. Theory*, **IT-29**, 521–535.
42. Drukarev, A. and Costello Jr, D. J. (1982) A comparison of block and convolutional codes in ARQ error control schemes. *IEEE Trans. Commun.*, **COM-30**, 2449–2455.
43. Lugand, L. and Costello Jr, D. J. (1982) A comparison of three hybrid ARQ schemes on a non-stationary channel. *Proc. GLOBECOM*, Miami, FL, pp. C8.4.1–C8.4.5.
44. Hagenauer, J. and Lutz, E. (1987) Forward error correction coding for fading compensation in mobile satellite channels. *IEEE J. Select. Areas Commun.*, **SAC-5**, 215–225.
45. Glisic, S. and Leppanen, P. (eds) (1997) *Wireless Communications; TDMA Versus CDMA*. London: Kluwer.

46. Saunders, S. (1999) *Antennas and Propagation for Wireless Communication Systems*. New York: John Wiley & Sons.
47. Winters, J. *et al*. (1994) The impact of antenna diversity on the capacity of wireless communication systems. *IEEE Trans. Commun.*, **42**(2–4), 1740–1750.
48. Marzetta, T. *et al*. (1999) Capacity of a mobile multiple-antenna communication link in Rayleigh flat fading. *IEEE Trans. Inform. Theory*, **45**(1), 139–157.
49. Foschini, G. *et al*. (1998) On the limit of wireless communication in a fading environment when using multiple antennas. *Wireless Personal Commun.*, **6**(3), 311–335.
50. Tarokh, V. *et al*. (1998) Space-time codes for high data rate wireless communication: performance criterion and code construction. *IEEE Trans. Inform. Theory*, **44**(2), 744–765.
51. Tarokh, V. *et al*. (1999) Space-time block codes from orthogonal design. *IEEE Trans. Inform. Theory*, **45**(5), 1456–1467.
52. *EURASIP J. Appl. Signal Process.*, Special issue on space-time coding and its applications-part I, **2002**(3), 2002.
53. Win, M. and Scholtz, R. (2000) Ultra-wide bandwidth time-hopping spread-spectrum impulse radio for wireless multiple access communications. *IEEE Trans. Commun.*, **48**(4), 679–689.
54. Win, M. and Scholtz, R. (1998) Impulse radio: how it works. *IEEE Commun. Lett.*, **2**(2), 36–38.
55. FCC (2002) *New Public Safety Applications and Broadband Internet Access Among Users Envisioned by FCC Authorization of Ultra Wideband Technology*. FCC first report and order, February 14, 2002, ET Docket No. 98–103, John Reed, jreed@fcc.gov. http://www.fcc.gov/Bureaus/Engineering_Technology/News-Releases/2002/nret0203.html.
56. Ramirez-Mireles, F. (2001) On the performance of ultra-wide-band signals in Gaussian noise and dense multipath. *IEEE Trans. Veh. Technol.*, **50**(1), 244–249.
57. Taylor, J. (ed.) (1995) *An Introduction to Ultra Wideband Radar Technology*. Boca Raton, FL: CRC Press.
58. *IEEE J. Select. Areas Commun.*, Special issue on "Software Radios", (4), 1999.
59. Pursley, M., Russell, H. and Wysocarski, J. (2000) Energy-efficient transmission and routing protocols for wireless multiple-hop networks and spread-spectrum radios. *EUROCOMM 2000, Information Systems for Enhanced Public Safety and Security, IEEE/AFCEA*, pp. 1–5.
60. McDonald, A. and Znati, T. (2000) A dual-hybrid adaptive routing strategy for wireless ad hoc networks. *IEEE Wireless Communications and Networking Conference, WCNC 2000*, Vol. 3, pp. 1125–1130.
61. Pursley, M., Russell, H. and Wysocarski, J. (2000) Energy-efficient routing in frequency-hop radio networks with partial-band interference. *IEEE Wireless Communications and Networking Conference, WCNC 2000*, Vol. 1, pp. 79–83.
62. Tien, T. C. and Upadhyaya, S. (2000) A local/global strategy based on signal strength for message routing in wireless mobile ad hoc networks 2000. *Proc. Academia/Industry Working Conference on Research Challenges*, pp. 227–232.
63. Tschudin, C., Lundgren, H. and Gulbrandsen, H. (2000) Active routing for ad hoc networks. *IEEE Commun. Mag.*, **38**(4), 122–127.
64. Garcia-Luna-Aceves, J. and Spohn, M. (1999) Efficient routing in packet-radio networks using link-state information. *IEEE Wireless Communications and Networking Conference*, Vol. 3, pp. 1308–1312.
65. Hettich, A. *et al*. (1999) Routing protocols for wireless ad hoc ATM networks. *2nd International Conference on ATM, ICATM '99*, pp. 49–58.
66. Ramanujan, R. *et al*. (1998) Source-initiated adaptive routing algorithm (SARA) for autonomous wireless local area networks. *Annual Conference on Local Computer Networks, LCN '98*, 23rd Proceedings, pp. 109–118.
67. Haas, Z. and Pearlman, M. (1998) The performance of a new routing protocol for the reconfigurable wireless networks. *IEEE International Conference on Communications*, *ICC '98 Conference Record*, Vol. 1, pp. 156–160.
68. Naghshineh, M. and Willebeek-LeMair, M. (1997) End to end QoS provisioning multimedia wireless/mobile networks using an adaptive framework. *IEEE Commun. Mag.*, **35**(11), 72–81.

69. Lin, C. *et al*. (1997) Adaptive clustering for mobile wireless networks. *IEEE J. Select. Areas Commun.*, **15**(7), 1265–1275.
70. Park, V. and Corson, M. (1997) A highly adaptive distributed routing algorithm for mobile wireless networks. *INFOCOM '97*, Proc. Vol. 3, pp. 1405–1413.
71. Gupta, P. and Kumar, P. (1997) A system and traffic dependent adaptive routing algorithm for ad hoc networks. *Proc. 36th IEEE Conference on Decision and Control*, Proc. Vol. 3, pp. 2375–2380.
72. Johnson, D. and Maltz, D. (1996) Truly seamless wireless and mobile host networking protocols for adaptive wireless and mobile networking. *IEEE Personal Commun.*, **3**(1), 34–42.
73. Roytblat, I. *et al*. (1996) Network connectivity buildup by adaptive learning. *19th Convention of Electrical and Electronics Engineers in Israel*, pp. 9–12.
74. Hortos, W. (1994) Application of neural networks to the adaptive routing control and traffic estimation of survivable wireless communication networks. *Southcon/94 Conference Record*, pp. 85–91.
75. *IEEE J. Select. Areas Commun.*, Special issue on "Active and programmable networks", **15**(3), 2001.
76. Hanzo, L. *et al*. (2002) *Adaptive Transceivers Communications*. New York: John Wiley & Sons.
77. 3GPP TS 25.308: UTRA High Speed Downlink Packet Access (HSDPA); overall description.
78. Glisic, S. and Leppanen, P. (eds) (1995) *Code Division Multiple Access Communications*. London: Kluwer.
79. Glisic, S. and Vucetic, B. (1997) *Spread Spectrum CDMA for Wireless Communications*. London: Artech House.
80. 3GPP TS 25.201: Physical layer – general description.
81. Holma, H. and Toskala, A. (2000) *WCDMA for UMTS*. New York: John Wiley & Sons.
82. Viterbi, A. J. (1995) *Principle of Spread Spectrum Communication*. Reading, MA: Addison-Wesley.
83. Prasad, R. (1996) *CDMA for Wireless Personal Communications*. London: Artech House.
84. 3GPP TS 25.101: UE Radio transmission and reception (FDD).
85. 3GPP TS 25.211: Physical channels and mapping of transport channels onto physical channels (FDD).
86. 3GPP TS 25.104: UTRA (BS) FDD; Radio transmission and reception.